Differences in Changes of the α1-β2 Subunit Contacts between Ligand Binding to the α and β Subunits of Hemoglobin A: UV Resonance Raman Analysis Using Ni−Fe Hybrid Hemoglobin†

Shigenori Nagatomo,§ Masako Nagai,# Naoya Shibayama,‡ and Teizo Kitagawa*,§

Center for Integrative Bioscience, Okazaki National Research Institutes, Myodaiji, Okazaki, Aichi 444-8585, Japan, and School of Health Sciences, Kanazawa University Faculty of Medicine, Kanazawa 920-0942, Japan, and Department of Physics, Jichi Medical School, Minamikawachi-machi, Kawachi-Gun, Tochigi 329-0498, Japan

Received January 16, 2002; Revised Manuscript Received May 2, 2002

ABSTRACT: The α1-β2 subunit contacts in the half-ligated hemoglobin A (Hb A) have been explored with ultraviolet resonance Raman (UVRR) spectroscopy using the Ni−Fe hybrid Hb under various solution conditions. Our previous studies demonstrated that Trpβ37, Tyrα42, and Tyrα140 are mainly responsible for UVRR spectral differences between the complete T (deoxyHb A) and R (COHb A) structures [Nagai, M., Wajcman, H., Lahary, A., Nakatsukasa, T., Nagatomo, S., and Kitagawa, T. (1999) *Biochemistry, 38,* 1243−1251]. On the basis of it, the UVRR spectra observed for the half-ligated $\alpha^{Ni}\beta^{CO}$ and $\alpha^{CO}\beta^{Ni}$ at pH 6.7 in the presence of IHP indicated the adoption of the complete T structure similar to $\alpha^{Ni}\beta^{deoxy}$ and $\alpha^{deoxy}\beta^{Ni}$. The extent of the quaternary structural changes upon ligand binding depends on pH and IHP, but their characters are qualitatively the same. For $\alpha^{Ni}\beta^{Fe}$, it is not until pH 8.7 in the absence of IHP that the Tyr bands are changed by ligand binding. The change of Tyr residues is induced by binding of CO, but not of NO, to the α heme, while it was similarly induced by binding of CO and NO to the β heme. The Trp bands are changed toward R-like similarly for $\alpha^{Ni}\beta^{CO}$ and $\alpha^{CO}\beta^{Ni}$, indicating that the structural changes of Trp residues are scarcely different between CO binding to either the α or β heme. The ligand induced quaternary structural changes of Tyr and Trp residues did not take place in a concerted way and were different between $\alpha^{Ni}\beta^{CO}$ and $\alpha^{CO}\beta^{Ni}$. These observations directly indicate that the phenomenon occurring at the α1-β2 interface is different between the ligand binding to the α and β hemes and is greatly influenced by IHP. A plausible mechanism of the intersubunit communication upon binding of a ligand to the α or β subunit to the other subunit and its difference between NO and CO as a ligand are discussed.

Human hemoglobin A (Hb A)[1] with an $\alpha_2\beta_2$ tetramer structure, exhibiting positive cooperativity in oxygen binding, has been extensively investigated, since it serves as a model of general allosteric proteins (*1*), and currently a route of communication from one to another subunit, which is the origin of cooperative ligand binding, is a major subject of Hb studies. X-ray crystallographic studies have demonstrated the presence of two distinct quaternary structures that correspond to the low-affinity (T or tense) and high-affinity (R or relaxed) states. Typical structures of the T and R states are seen for the complete deoxy and liganded forms, respectively (*2*). The cooperative oxygen binding of Hb has been explained in terms of a reversible transition between the two quaternary states on partial ligation of four hemes (*3*, *4*). The largest structural differences between the T and R states, revealed by X-ray crystallographic analysis (*5*), are located in the α1-β2 subunit interface, where resets of hydrogen bonds and cleavage of salt-bridges take place upon ligation to deoxyHb. The ^{1}H NMR signal of Tyrα42, which forms a hydrogen bond with Aspβ99 in the T state but is free in the R state, has served as a practical diagnostic marker for the quaternary structure (*6*, *7*), although a single marker is not sufficient to characterize the quaternary state.

If the two-state model described above is correct, all residues at the α1-β2 interface should change in a concerted way at the crossover point of the T and R states. To investigate protein structures in intermediate states of ligand binding to Hb A, a variety of metal substituted Hbs including their hybrid has been prepared with Ni, Co, Cu, Cr, Zn, Mn, Mg, and so on (*8*−*18*). The Co substituted Hb can bind O_2 with lower affinity than Hb A by a factor of 10, but cannot bind CO (*10*). The subunit substituted with other metal

† This work was supported by Grant-in-Aid from the Ministry of Education, Culture, Sports, Science and Technology, Japan, to M.N. (10670115) and T.K. (12045264).

* To whom correspondence should be addressed: phone: 81-564-59-5225, fax: 81-564-59-5229, e-mail: teizo@ims.ac.jp.

§ Okazaki National Research Institutes.

Kanazawa University Faculty of Medicine.

‡ Jichi Medical School.

[1] Abbreviations: Hb A, hemoglobin A; COHb A, carbonmonoxy Hb A; IHP, inositol-hexa(kis)phosphate; RR, resonance Raman; UVRR, ultraviolet resonance Raman; $\alpha^{Ni}\beta^{deoxy}$, α(Ni)β(Fe-deoxy)Hb A; $\alpha^{Ni}\beta^{CO}$, α(Ni)β(Fe−CO)Hb A; $\alpha^{deoxy}\beta^{Ni}$, α(Fe-deoxy)β(Ni)Hb A; $\alpha^{CO}\beta^{Ni}$, α(Fe−CO)β(Ni)Hb A; $\alpha^{Ni}\beta^{O2}$, α(Ni)β(Fe−O_2)Hb A; $\alpha^{O2}\beta^{Ni}$ Hb A, α(Fe−O_2)β(Ni)Hb A; Ni-PPDME; Ni-protoporphyrin IX dimethylester; $\alpha^{NO}\beta^{deoxy}$, α(Fe−NO)β(Fe-deoxy)Hb A; $\alpha^{NO}\beta^{CO}$, α(Fe−NO)β(Fe−CO)Hb A; NOHb A, nitrosyl Hb A; NOMb, nitrosyl myoglobin; THF, tetrahydrofuran; TPP, tetraphenyl-porphyrin.

10.1021/bi0200460 CCC: $22.00
Published on Web 07/11/2002

species cannot bind even O_2. Accordingly, hybrid Hbs with Fe and another metal can generate the half-liganded intermediate with two ligands on the Fe subunits. A quaternary structure of the half liganded Hb depends on the metal species hybridized. Physicochemical properties of Ni−Fe hybrid Hb changes with whether Ni is incorporated into the α ($\alpha^{Ni}\beta^{Fe}$) or β ($\alpha^{Fe}\beta^{Ni}$) subunit (*8*, *9*, *16*−*18*). X-ray crystallographic analysis demonstrated that both $\alpha^{Ni}\beta^{CO}$ (*16*) and $\alpha^{O2}\beta^{Ni}$ (*17*) maintain the T structure at pH 6.8 even in the ligand-bound state. The ^{1}H NMR measurements on the Ni−Fe hybrid Hb revealed appreciable pH dependence. At pH 7.4 in the presence of IHP both $\alpha^{Ni}\beta^{CO}$ and $\alpha^{CO}\beta^{Ni}$ gave the ^{1}H signals of Tyrα42 and Trpβ37, which mean the presence of the T-type α1-β2 contact. As the pH was raised, intensities of these signals became weaker, and the extent of weakening was definitely different between Tyrα42 and Trpβ37 for $\alpha^{Ni}\beta^{CO}$ but not always so for $\alpha^{CO}\beta^{Ni}$. This suggests that the structural changes of Tyrα42 and Trpβ37 are not synchronous in $\alpha^{Ni}\beta^{CO}$ (*9*). The absorption spectra of $\alpha^{Ni}\beta^{CO}$ suggested a pH-dependent change for a coordination number of Ni; four at pH 6.5 and five at pH 8.5. Presumably, proximal Hisα87 is coordinated to Ni at pH 8.5 but is dissociated at pH 6.5, while His is always coordinated to Ni in the β heme (*8*). The great difference between the α and β subunits is also incompatible to the two-state model. Previously, we examined UV resonance Raman (UVRR) spectra of α-nitrosyl β-deoxy Hb A ($\alpha^{NO}\beta^{deoxy}$) and pointed out its structural change upon ligation to the deoxyFe subunit (*19*). In an extension of the investigation of the α1-β2 contacts in partially liganded Hb, which can be different between α- or β-ligation, we treated Ni−Fe hybrid Hb in this study.

It has been demonstrated in this decade that resonance Raman (RR) spectra excited in the UV region around 220−240 nm can explore the environmental and hydrogen-bonding changes of Tyr and Trp residues of proteins (see refs *20* and *21* for a review). In fact, Rodgers et al. (*22*, *23*), Nagai, M., et al. (*24*−*26*), Huang et al. (*27*, *28*), Hu et al. (*29*, *30*), and Peterson and Friedman (*31*) reported the quaternary structure dependent features for Tyr and Trp residues in the α1-β2 interface of Hb using 230- and 235-nm excited UVRR spectra. The quaternary structure dependent UVRR bands have been assigned to Trpβ37, Tyrα42, and Tyrα140 (*24*−*26*). Here we present 235-nm excited UVRR spectra for $\alpha^{Ni}\beta^{deoxy}$, $\alpha^{Ni}\beta^{CO}$, $\alpha^{deoxy}\beta^{Ni}$, and $\alpha^{CO}\beta^{Ni}$ in the presence and absence of IHP at various pH values, discussing differences in a communication route between the α to β subunits and the β to α subunits, and also possible correlation between the Fe−His bonding of α hemes and intersubunit interactions at the α1-β2 interface in the quaternary structure change.

EXPERIMENTAL PROCEDURES

Sample Preparation. Hb A was purified from fresh human blood by a preparative isoelectric focusing electrophoresis (*32*). Approximately 150 μL of the 200 μM (in terms of heme) Hb A solution was put into a spinning cell made of a synthetic quartz ESR tube (diameter = 5 mm) (*33*). DeoxyHb and COHb were prepared by adding sodium dithionite (1 mg/mL) to oxyHb after replacement of the inside air of the sample tube with N_2 and CO, respectively. Ni−Fe hybrid Hb was prepared as described previously (*8*). The $\alpha^{Ni}\beta^{deoxy}$ and $\alpha^{deoxy}\beta^{Ni}$ were generated from $\alpha^{Ni}\beta^{CO}$ and $\alpha^{CO}\beta^{Ni}$, respectively, by photodissociation of CO under flowing of O_2, followed by addition of sodium dithionite (1 mg/mL) under N_2 atmosphere. The $\alpha^{Ni}\beta^{CO}$ and $\alpha^{CO}\beta^{Ni}$ used for UVRR measurements were obtained by addition of CO to the $\alpha^{Ni}\beta^{deoxy}$ and $\alpha^{deoxy}\beta^{Ni}$ thus generated. Solvents used were phosphate buffer for the pH range from pH 6.7 to 7.4, Tris buffer at pH 8.1, and borate buffer at pH 8.7. IHP was added to the samples, when necessary, with a final concentration of 5 mM. Ni-PPDME was a kind gift of Prof. H. Ogoshi (*34*).

Ultraviolet Resonance Raman Measurements. Just before the measurement of the UVRR spectra, Na_2SO_4 was added to the samples with the final concentration of 0.1 M as an internal intensity standard for Raman spectra. It was confirmed that the addition of sulfate did not cause any apparent Raman spectral change for the states examined in this study, although its use in Raman experiments was warned against due to a possible tertiary structure change (*35*). UVRR spectra were excited by a XeCl excimer laser-pumped dye laser (EMG103MSC/LPX120 and FL2002/SCANMATE, Lambda Physik). The 308-nm line from the XeCl excimer laser (operated at 100 Hz) served as a pump to excite coumarin 480, and the 470-nm output from the dye laser was frequency-doubled with a β-BaB_2O_4 crystal to generate 235-nm pulses. The Raman excitation light (15 μJ/pulse) with the cross section of 0.2 × 3 mm^2 was introduced to a sample cell from the lower front side. Scattered light at the scattering angle of 135° was dispersed with an asymmetric double monochromator (Spex 1404) in which the gratings in the first and second dispersion steps were 2400 grooves/mm (holographic) and 1200 grooves/mm (machine-ruled, 500 nm blazed), respectively (*36*), and detected by an intensified photodiode array (PC-IMD/C5222-0110G).

The spinning cell was moved vertically by 1 mm for every spectrum (every 5 min) to shift the laser illumination spot on the sample (*33*). The temperature of the sample solution was kept at 10 °C by flushing with cooled N_2 gas against the cell. The scattered light was collected with Cassegrainian optics with f/1.1. One spectrum is composed of the sum of 400 exposures, each exposure accumulating the data for 0.8 s. The Raman spectra shown in the figure are averages of 10 or 15 spectra. Raman shifts were calibrated with cyclohexane. Raman intensity was standardized with the band intensity of sulfate ions at 982 cm^{-1}. Denaturation of the samples due to exposure to UV laser light was carefully checked by inspecting a possible change in the visible absorption spectra before and after the measurements of UVRR spectrum. If some spectral changes were noticed, the Raman spectrum was discarded. Visible absorption measurements were carried out with a Hitachi 220S spectrophotometer.

Visible Resonance Raman Measurements. The 441.6 nm line from a He/Cd laser (model CD4805R, Kimmon Electrics Corp.) was used as an excitation source. Visible resonance Raman scattering was detected with a liquid nitrogen-cooled CCD detector (model CCD3200, Astromed) attached to a 100-cm single polychromator (model MC-100DG, Ritsu Oyo Kogaku). The slit width and slit height were set to be 200 μm and 10 mm, respectively. The corresponding spectral slit width is 8 cm^{-1}. The wavenumber width per one channel of the detector was 0.7 cm^{-1}. The laser power used was 5.4

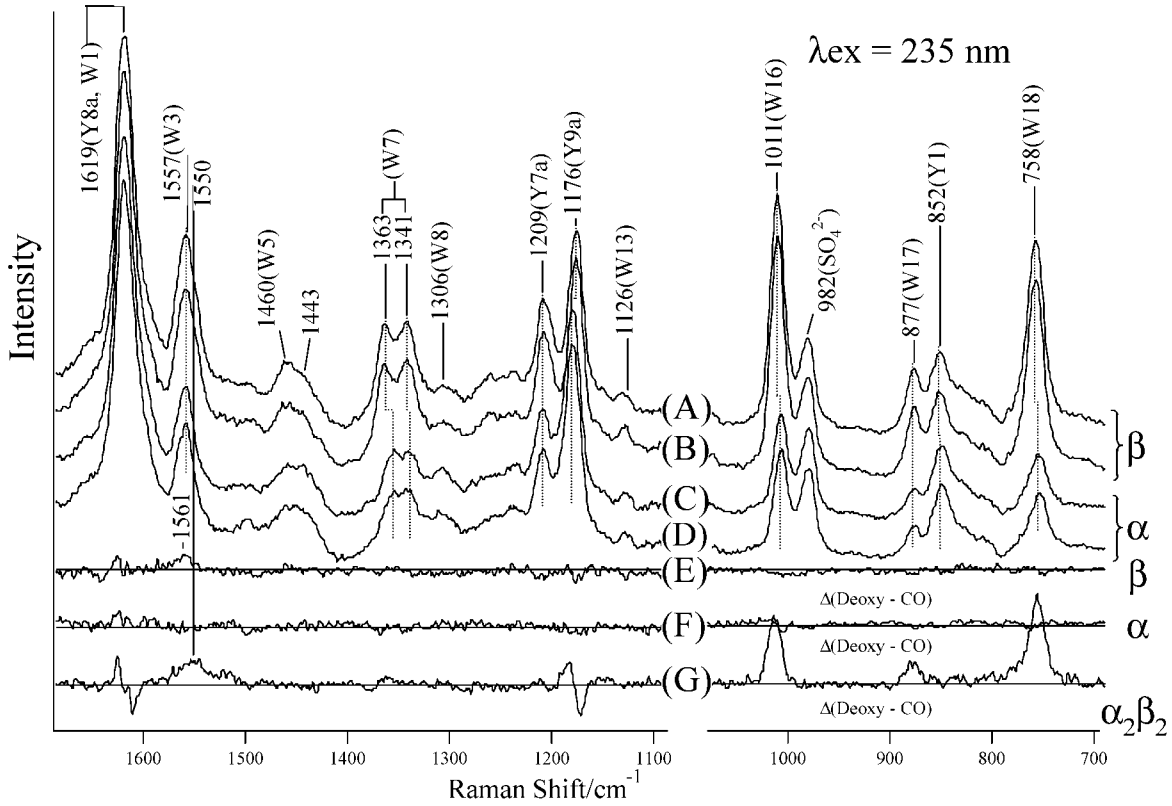

FIGURE 1: The 235-nm excited UVRR spectra of the isolated β-chain in the deoxy (A) and CO-bound (B) forms, the isolated α-chain in the deoxy (C) and CO-bound (D) forms and the deoxy-minus-CO difference spectra for the isolated β (E) (= A − B) and α-chains (F) (= C − D), and native Hb A (G). All samples are equilibrated with 0.05 M phosphate buffer, pH 6.7, containing 0.1 M Na_2SO_4, and protein concentrations were 200 μM in heme. Each spectrum is an average of 10 or 15 spectra. The ordinate scales of the difference spectra are the same as those of raw spectra. The band marked by SO_4^{2-} means the totally symmetric stretching band of SO_4^{2-} ions.

mW at the sample point. All measurements were carried out at room temperature with a spinning cell (1000 rpm). Raman shifts were calibrated with indene and accuracy of peak positions of Raman bands was ±1 cm^{-1}.

RESULTS

UVRR Spectra of the Isolated α and β Chains and $\alpha_2\beta_2$ Tetramer. Figure 1 shows the 235-nm excited UVRR spectra of the isolated β-chain in the deoxy (A) and CO-bound (B), and the isolated α chain in the deoxy (C) and CO-bound (D) states at pH 6.7 in the frequency region from 1700 to 700 cm^{-1} and the deoxy-minus-CO difference spectra for the isolated β (E) and α (F) chains and native Hb A (G). Although a strong broad band due to a synthetic quartz cell appeared between 800 and 900 cm^{-1}, its contribution was subtracted from the spectra shown here. The 982 cm^{-1} band of SO_4^{2-} ions was used to normalize the intensity of the spectra, as their presence did not affect the observed spectra (*37*). In the spectrum of the β-deoxy chain (A), RR bands of tyrosine (Tyr) are seen at 1619 (Y8a), 1209 (Y7a), 1176 (Y9a), and 852 cm^{-1} (Y1), and those of tryptophan (Trp) are seen at 1619 (W1, overlapped), 1557 (W3), 1363−1341 (W7; tryptophan doublet), 1011 (W16), 877 (W17), and 758 cm^{-1} (W18). The assignments are based on Harada and coworkers (*20*, *38*, *39*). The UVRR spectra of deoxyHb A and COHb A in the 1700−850 cm^{-1} (not shown) are in agreement with those reported by Rodgers et al. (*22*) and Nagai et al. (*24*, *26*). It was confirmed that the spectra of deoxyHb A and COHb A exhibited negligible changes upon addition of IHP (spectra not shown).

The Raman scattering from Trp residues is stronger for the β-deoxy chain than for the α-deoxy chain due to the number of residues (two in the β-chain and one in the α-chain). The peak frequencies of the W7, W16, and W18 bands are slightly different between the isolated α- and β-chains. Digital sum of the UVRR spectra of the α-CO and the β-CO chains almost coincides with the spectrum observed for native COHb A, but the corresponding digital sum of the α-deoxy and the β-deoxy chains is slightly but definitely different from the spectrum observed for native deoxyHb A. The difference lies mainly in the intensity of Trp bands, suggesting that the surroundings of Trp residues are unique in the T-structure tetramer but not so in the R-structure tetramer. The intensity increase of Trp bands in the 235 nm-excited UVRR spectrum is generally ascribed to a shift of the B_b absorption maximum to a longer wavelength and thus to the increase of hydrophobicity around the indole ring (*40*) or the formation of a hydrogen bond at the indole NH site in hydrophobic environments (*41*). Such differences of Trp residue between the α (or β) oligomers and the $\alpha_2\beta_2$ tetramer would occur more easily to a Trp residue on the contact surfaces of subunits than that in the interior of individual subunits. Consequently, it is quite reasonable that the Trp residue responsible for the difference peak in the deoxy-minus-CO difference spectrum is mainly Trpβ37 rather than Trpβ15 and Trpα14.

The Tyr spectrum of the isolated β chain also differs from that of the isolated α chain. The frequency of the Y9a band of the β-deoxy chain is lower than that of the α-deoxy chain by as much as 4 cm^{-1}, although the frequencies are unaltered

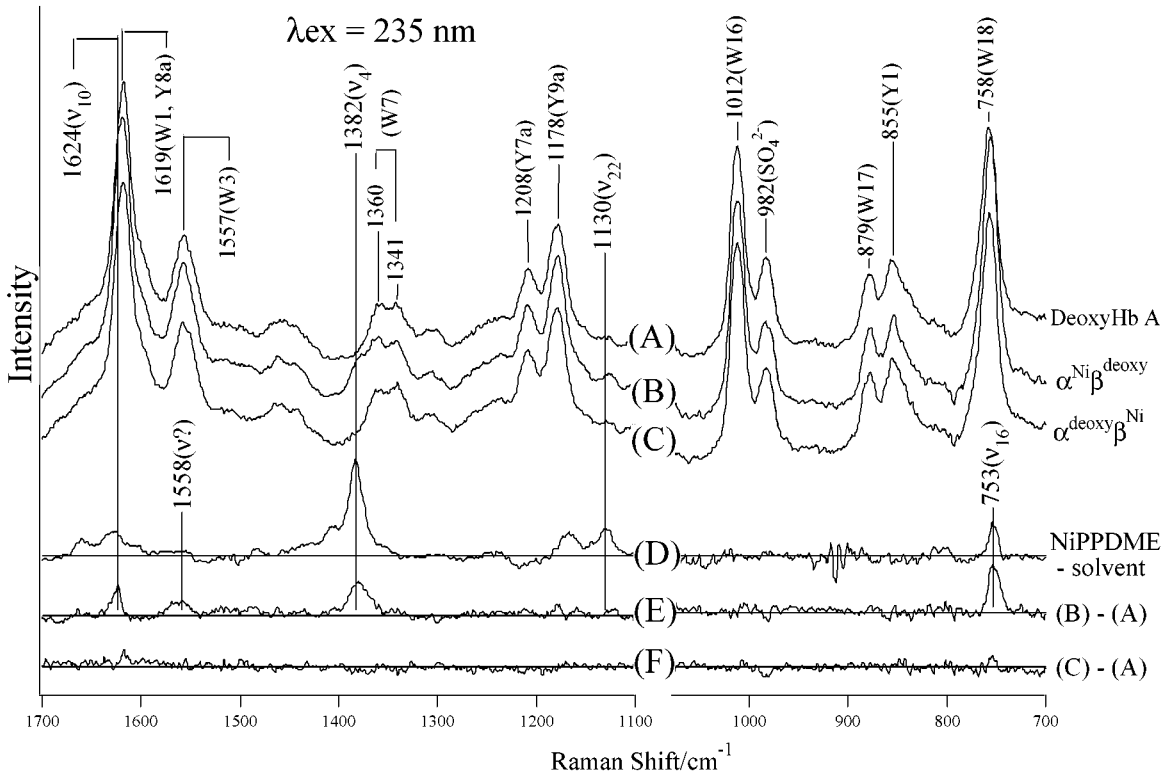

FIGURE 2: The 235-nm excited UVRR spectra of deoxyHbA (A), $\alpha^{Ni}\beta^{deoxy}$(+IHP) (B), $\alpha^{deoxy}\beta^{Ni}$(+IHP) (C) and Ni-PPDME (D), and their difference spectra of $\alpha^{Ni}\beta^{deoxy}$ (+IHP) − deoxyHbA (E), and of $\alpha^{deoxy}\beta^{Ni}$ (+IHP) − deoxyHbA (F). All Hb samples are equilibrated with 0.05 M phosphate buffer, pH 6.7, containing 0.1 M Na_2SO_4 and 5 mM IHP. Hb concentration was 200 μM in heme. Ni-PPDME concentration was 20 mM (in $CHCl_3$, 1100−1700 cm^{-1}) or 0.6 mM (in THF, 700−1100 cm^{-1}). Each Hb spectrum is an average of 10 spectra. The spectrum of Ni-PPDME is an average of four spectra and the contribution from solvents have been subtracted. The ordinate scales of the difference spectra are the same as those of raw spectra. The band marked by SO_4^{2-} means the totally symmetric stretching band of SO_4^{2-} ions.

by CO binding within the α (or β) oligomers. This means that the surroundings of Tyr in the α-deoxy chain are more hydrophilic than that in the β-deoxy chain. This spectral difference may be related to the status difference between the α- and β-chains, that is, a dimer for the α and a tetramer for the β-chains.

The deoxy-minus-CO difference spectrum of the isolated α-chain (F) exhibits no peak, indicating that the surroundings around Tyr and Trp are scarcely altered by the tertiary structure change induced by the ligand binding. The corresponding difference spectrum of the isolated β-chain (E) also exhibits no peak except for a small peak due to the Trp W3 band at 1561 cm^{-1}. Note that these reflect the extent of contributions to the UVRR spectral changes from the tertiary structure change in oligomers of isolated chains upon the ligand binding. It is known that the W3 frequency reflects the torsion angle around the $C_2-C_3-C_\beta-C_\alpha$ linkage of Trp (*30*, *39*).

The difference spectrum between deoxyHb A and COHb A (G) indicates that the intensities of the W3, W16, W17, and W18 bands of Trp are much weaker for COHb A than for deoxyHb A, while the peak positions remain unaltered except for the W3 band, and that the frequencies of Y8a and Y9a bands of Tyr are lower for COHb A than for deoxyHb A. These differences arise from some differences in hydrogen bonding states and surrounding hydrophobicity of mainly Trpβ37, Tyrα42, and Tyrα140 residues between the two states (*26*, *42*) and have been ascribed to a consequence of changes in subunit contacts (*22*−*31*, *43*). It was pointed out previously by Rodgers (*22*) and Hu and Spiro (*29*) that the $C_2-C_3-C_\beta-C_\alpha$ torsion angle of Trpβ37 is smaller than those of Trpα14 and Trpβ15 for Hb A, and, accordingly, its W3 frequency is lower than others.Therefore, the difference peak at 1550 cm^{-1} is ascribed to Trpβ37. The absence of this peak in the spectra for the isolated chains may mean that the smaller torsion angle is specific to the $\alpha_2\beta_2$ tetramer.

It is evident that the spectral sum of the deoxy-minus-CO differences of the isolated α- and β-chains does not yield the deoxy-minus-CO difference spectrum of the $\alpha_2\beta_2$ tetramer having a special contact at the α1-β2 subunit interface. This demonstrates that the UVRR spectral differences shown by trace G reflect mostly the quaternary structure change, but not the tertiary one. Hereafter, spectrum (G) will be referred as the standard for the T-minus-R difference spectrum, reflecting 100% changes at the α1-β2 subunit interface due to the quaternary structure transition ("T-like" and "R-like" will be used to represent that the local structure around a particular residue in question is closer to that in the ordinary T and R subunit contact, respectively, but does not always mean that the whole tetramer structure is close to the T and R, respectively).

Figure 2 compares the spectra of Ni−Fe hybrid Hb (B and C) with those of Hb A (A) in the deoxy state. The spectrum of $\alpha^{Ni}\beta^{deoxy}$ (B) is different from that of deoxyHb A (A), although the spectrum of $\alpha^{deoxy}\beta^{Ni}$ (C) is not so. The difference spectrum for the α subunit (E), $\alpha^{Ni}\beta^{deoxy}$ − deoxyHb A, yields positive peaks at 1624(ν_{10}), 1382(ν_4), 1130(ν_{22}), and 753(ν_{16}) cm^{-1}, while the difference spectrum for the β subunit (F), $\alpha^{deoxy}\beta^{Ni}$ − deoxyHb A, yielded no

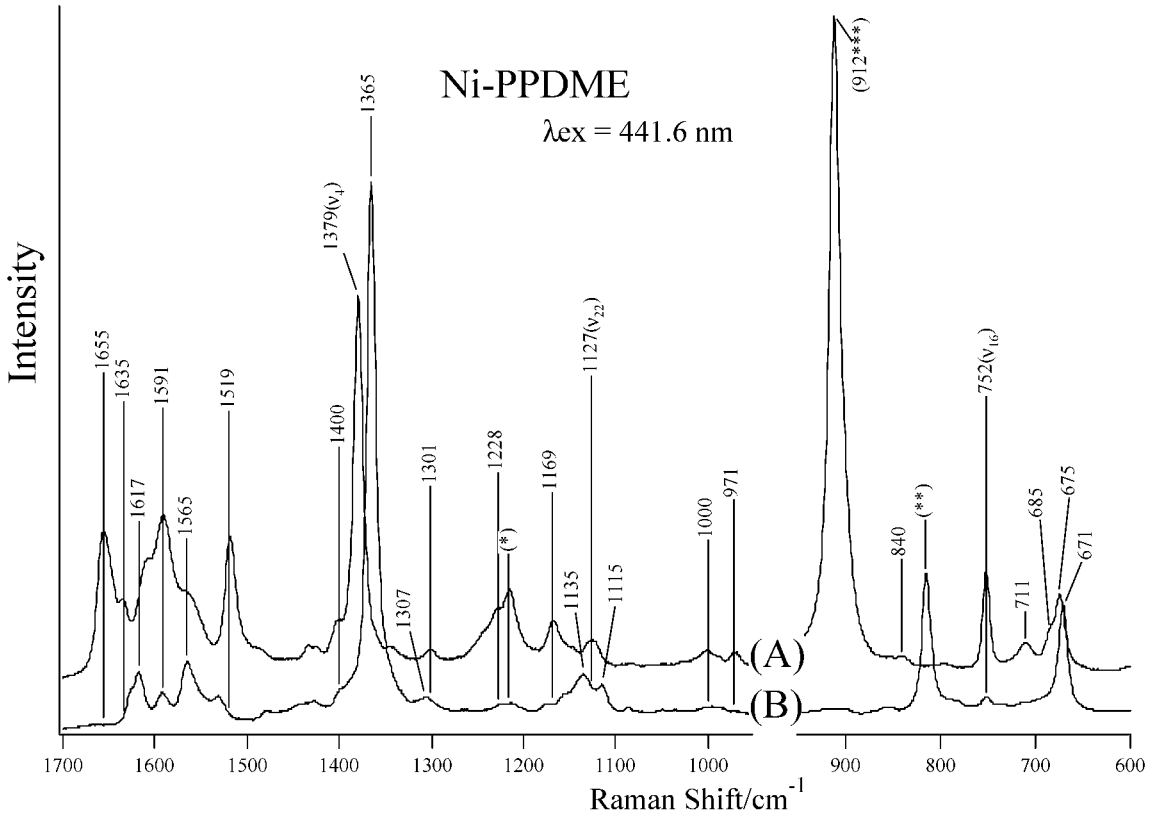

FIGURE 3: The 441.6-nm excited RR spectra of Ni-PPDME in $CHCl_3$ (1700−950 cm^{-1}) or THF (950−600 cm^{-1}) (A), and in piperidine (B). Ni-PPDME concentration was 100 μM (in $CHCl_3$ or THF) and 150 μM (in piperidine). The bands marked by *, **, and *** mean bands of $CHCl_3$, piperidine, and THF, respectively.

peaks. These peaks are not present in spectrum (A) and are ascribed to porphyrin vibrations, because the peak positions are the same as those of four-coordinated Ni-protoporphyrin, whose spectrum excited at 235 nm is delineated by spectrum (D). The mode numbers of porphyrin vibrations (*44*, *45*) are specified in parentheses. The absence of the corresponding peaks in trace (F) means that the Ni-porphyrin in the β subunit adopts the five-coordinate structure, yielding no prominent Raman bands upon excitation at 235 nm.

Figure 3 shows the visible-excited RR spectra of four-coordinated Ni−PPDME (A) in $CHCl_3$ (1750−950 cm^{-1}) or THF (950−600 cm^{-1}) and six-coordinated Ni-PPDME (B) in piperidine. The ν_{16} band at 752 cm^{-1} is very weak for six-coordinated Ni-PPDME (B) compared with that for four-coordinated one (A). Accordingly, the 753 cm^{-1} band in Figure 2E is assigned to the ν_{16} mode of the four-coordinated α(Ni) heme. Similarly, the 1382 cm^{-1} band in Figure 2E corresponds to the ν_4 (1379 cm^{-1}) band in Figure 3A, whose frequency depends on the coordination number, and is ascribed to the four-coordinated α(Ni) heme. Thus, some caution is necessary to distinguish between the UVRR bands of Ni-porphyrin and of globin, particularly for $\alpha^{Ni}\beta^{deoxy}$.

UVRR Spectra of $\alpha^{Ni}\beta^{CO}$ *Hybrid Hb.* Figure 4 shows the raw UVRR spectrum of $\alpha^{Ni}\beta^{CO}$ (A) at pH 6.7 in the presence of IHP and the difference spectra between $\alpha^{Ni}\beta^{deoxy}$ and $\alpha^{Ni}\beta^{CO}$ at various pH values in the presence or absence of IHP in the frequency region from 1700 to 700 cm^{-1}. The general trend of these difference spectra for $\alpha^{Ni}\beta^{Fe}$ is that peak intensities in the difference spectra increase when proceeding from spectra (B) to (H); that is, more R-like contacts are promoted in the ligand bound form of the β subunit at higher pH. Detailed analysis, however, clarifies that the Tyr and Trp bands do not change in a concerted way. The first change to the R-type occurs only on the Trp bands in spectrum (C) at pH 6.7 in the absence of IHP, although there is no difference in its presence (B). It is stressed that the change to the R-type is not observed at all for Tyr bands even at pH 7.1 in the presence of IHP (D), which is almost the same as spectrum (C). At pH 8.1 in the presence of IHP (F), small changes of Tyr bands to R-like are recognized, while the changes of Trp bands to the R-type proceed. It is not until pH 8.7 in the absence of IHP (G) that the changes of Tyr bands to the R-type become evident, although it is still smaller than that of normal Hb A, which is depicted by spectrum (H) for comparison.

UVRR Spectra of $\alpha^{CO}\beta^{Ni}$ *Hybrid Hb.* Figure 5 shows the raw UVRR spectrum of $\alpha^{CO}\beta^{Ni}$ (A) in the frequency region from 1700 to 700 cm^{-1} and the difference spectra between $\alpha^{deoxy}\beta^{Ni}$ and $\alpha^{CO}\beta^{Ni}$ at various pH values in the presence and absence of IHP. The R-like contacts at the subunit interface due to ligand binding to the α subunit are promoted by raising pH, and thus difference peaks are intensified. In this context, the general trend of the difference spectra for $\alpha^{CO}\beta^{Ni}$ Hb are similar to those of $\alpha^{Ni}\beta^{CO}$, although in delicate points the behaviors of $\alpha^{CO}\beta^{Ni}$ and $\alpha^{Ni}\beta^{CO}$ are different from each other. A large difference between them is that changes of Tyr bands toward the R-type occurs in the earlier stage: it is already seen in the spectrum at pH 6.7 in the absence of IHP (C). At the same pH, however, the Tyr bands are not discernible in the presence of IHP (B). The size of change of Tyr bands is nearly full at pH 6.7 in the absence of IHP

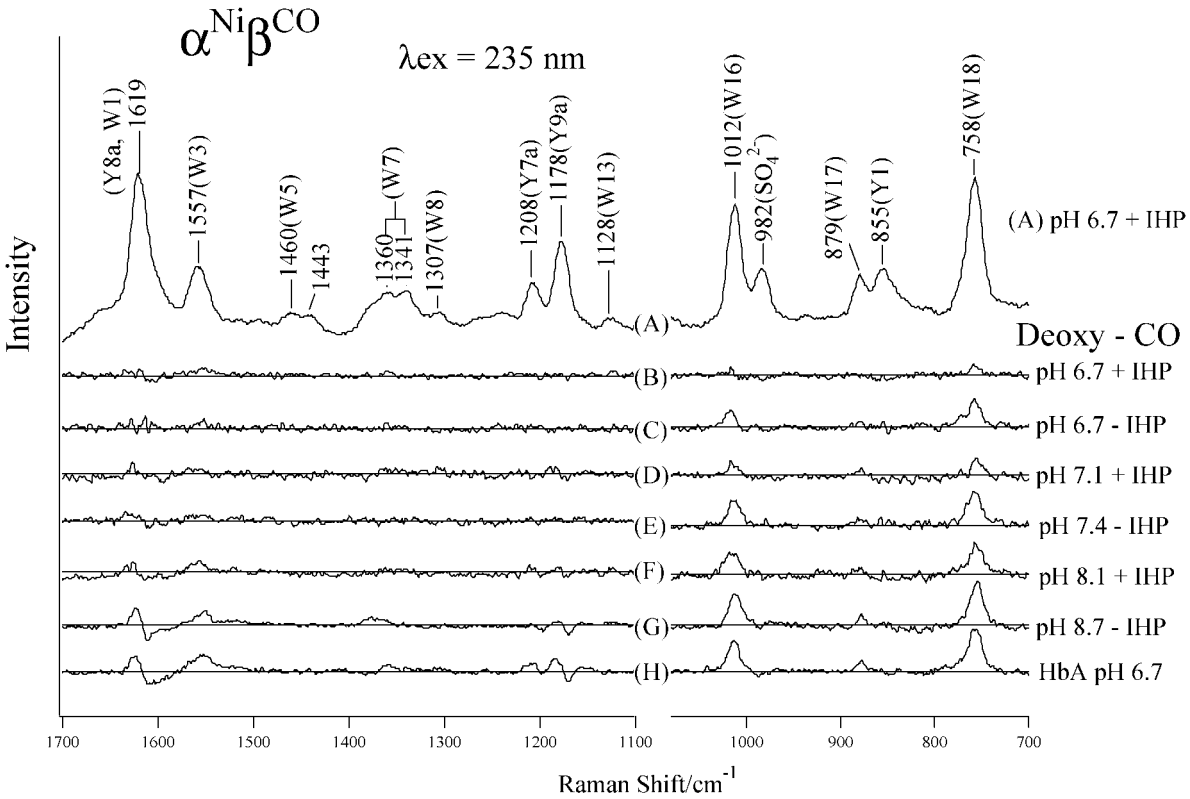

FIGURE 4: UVRR spectrum of $\alpha^{Ni}\beta^{CO}$ at pH 6.7 (+IHP) (A) and the difference spectra of $\alpha^{Ni}\beta^{deoxy} - \alpha^{Ni}\beta^{CO}$ at pH 6.7 (+IHP) (B), pH 6.7 (−IHP) (C), pH 7.1 (+IHP) (D), pH 7.4 (−IHP) (E), pH 8.1 (+IHP) (F), and pH 8.7 (−IHP) (G) and deoxyHbA − COHbA at pH 6.7 (H). Hb concentration was 200 μM in heme. Each Hb spectrum is an average of 10 or 15 spectra. The ordinate scales of the difference spectra are the same as those of raw spectra. The band marked by SO_4^{2-} means the totally symmetric stretching band of SO_4^{2-} ions. Normal HbA samples are equilibrated with 0.05 M phosphate buffer, pH 6.7, containing 0.1 M Na_2SO_4. All $\alpha^{Ni}\beta^{CO}$ samples are equilibrated with 0.05 M phosphate, Tris or borate buffer, containing 0.1 M Na_2SO_4. The IHP concentration was 5 mM when it was contained. The difference spectra were obtained by subtraction of the spectrum of each CO form at the same pH in the absence of IHP from the spectrum of designated sample.

(C), while the spectral changes of Trp bands toward the R-type are still on going. In the presence of IHP, the change of Tyr bands are not so clear even at pH 7.2 (D), where the change of Trp bands proceeds to the level of 40−50% R-like, similar to the case of pH 6.7 in the absence of IHP (C). Thus, it is evident that *IHP has a propensity to keep Tyr in the T-like contact but not so for Trp*. The difference spectrum at pH 8.7 in the absence of IHP (F) exhibits the same spectrum as that for normal Hb A, which is delineated by spectrum (G) for comparison. The changes of Tyr and Trp to R-like upon CO binding to the deoxy-heme of $\alpha^{deoxy}\beta^{Ni}$ were observed in a manner different from the case for $\alpha^{Ni}\beta^{deoxy}$. Moreover, a size of the T to R spectral change for Trp seems to be somewhat smaller in $\alpha^{CO}\beta^{Ni}$ than that in $\alpha^{Ni}\beta^{CO}$ under the same conditions.

DISCUSSION

Differences in Structural Changes between Ligand Binding to the α and β Subunits. The CO-bound forms of Ni−Fe hybrid Hb serve as a good model for studying a structure of half-liganded Hb which is not stable in the normal Hb A, because Ni-porphyrins cannot bind O_2 and CO. The function and structure of the Ni−Fe hybrid Hb have been extensively studied (*8*, *9*, *16*−*18*), and in the present experiments we have detected conformational changes of the protein moiety of the Ni−Fe hybrid Hb with 235-nm excited UVRR spectroscopy, which provides strong enhancement of Raman intensity for vibrational modes associated with Tyr and Trp residues. DeoxyHb A gives a typical UVRR spectrum of the T-structure which is distinct from the spectrum of COHb A with the R-structure. These two spectra will be referred as the standard in the analysis below. When the ligand binding to the deoxy-Fe heme caused shifting of the α1-β2 contact toward more R-like, peak intensity in the deoxy-minus-CO difference spectrum approaches more to that in the deoxyHb A-minus-COHb A difference spectrum.

It was demonstrated in Figure 1 that Tyr and Trp residues in the isolated α- or β-chains exhibited almost no changes in their structure and environments between the deoxy- and CO-forms unless the particular contact at the α1-β2 interface was attained in the $\alpha_2\beta_2$ tetramer. The Ni−Fe hybrid Hb at pH 6.7 in the presence of IHP gave the T-like spectrum regardless of CO binding to the Fe subunit, being consistent with ^{1}H NMR studies (*9*). The fact that the UVRR spectra of $\alpha^{Ni}\beta^{CO}$ and $\alpha^{CO}\beta^{Ni}$ are hardly different from those of $\alpha^{Ni}\beta^{deoxy}$ (Figure 4B) and $\alpha^{deoxy}\beta^{Ni}$ (Figure 5B), respectively, means that Tyr and Trp residues do not undergo any changes by CO binding in the presence of IHP at pH 6.7. These residues exhibit appreciable changes upon CO binding to the Fe subunit at higher pH. The most interesting point in the results of the Ni−Fe hybrid Hb is that a pattern of quaternary structural change is different between the CO binding to the α and β hemes. It means that the communication route from the α to β subunit is different from the corresponding route from the β to α subunit.

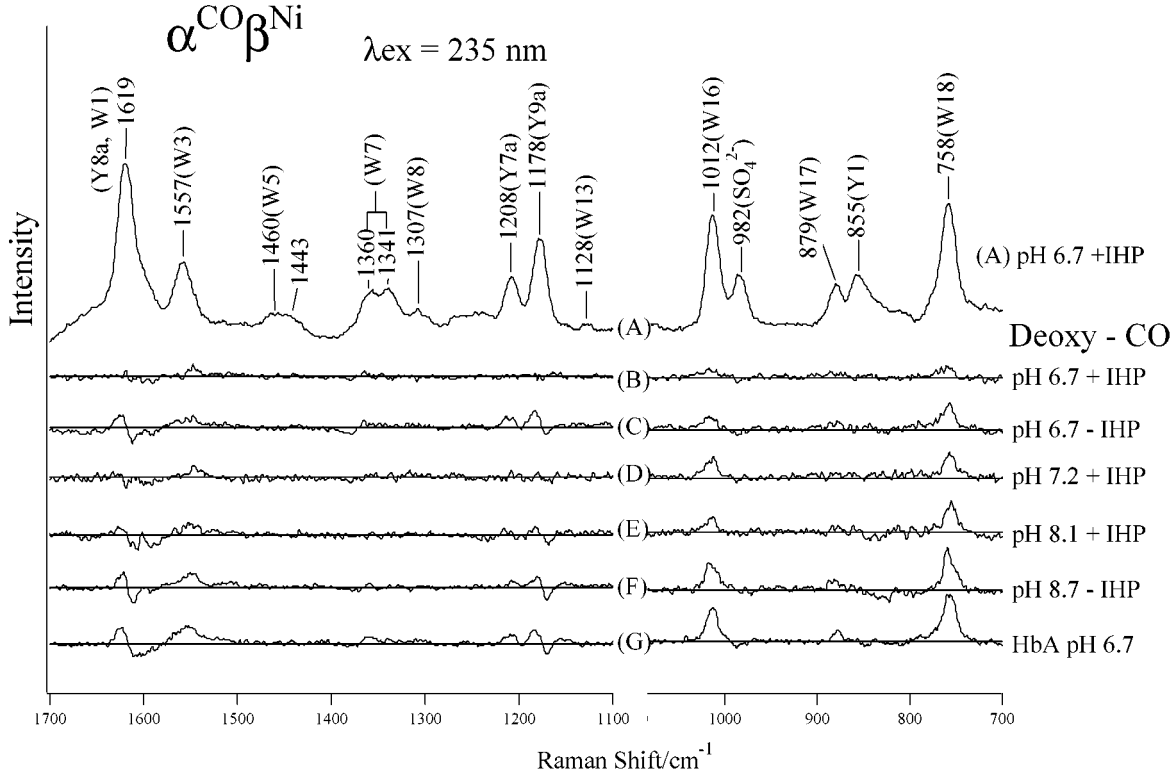

FIGURE 5: UVRR spectrum of $\alpha^{CO}\beta^{Ni}$ at pH 6.7 (+IHP) (A), and the difference spectra of $\alpha^{deoxy}\beta^{Ni} - \alpha^{CO}\beta^{Ni}$ at pH 6.7 (+IHP) (B), pH 6.7 (−IHP) (C), pH 7.2 (+IHP) (D), pH 8.1 (+IHP) (E), and pH 8.7 (−IHP) (F), and of deoxyHbA − COHbA at pH 6.7 (G). Hb concentration was 200 μM in heme. Each Hb spectrum is an average of 10 or 15 spectra. The ordinate scales of the difference spectra are the same as those of raw spectra. The band marked by SO_4^{2-} means the totally symmetric stretching band of SO_4^{2-} ions. Normal HbA samples are equilibrated with 0.05 M phosphate buffer, pH 6.7, containing 0.1 M Na_2SO_4. All $\alpha^{CO}\beta^{Ni}$ samples are equilibrated with 0.05 M phosphate, Tris or borate buffer, containing 0.1 M Na_2SO_4. The IHP concentration was 5 mM when it was contained. The difference spectra were obtained by subtraction of the spectrum of each CO form at the same pH in the absence of IHP from the spectrum of designated sample.

Binding of CO to $\alpha^{Ni}\beta^{deoxy}$, which is expected to reveal the route from the β to the $\alpha1$-$\beta2$ interface, mainly induced the subunit contact change of Trp residues toward R-like, that is summarized as follows. As the pH is raised, the population of R-like contacts of Trp becomes more dominant. IHP has an effect to maintain the T-like contacts at lower pH (<pH 6.7), but no effect at higher pH (>pH 8.1). It is not until pH 8.7 in the absence of IHP (Figure 4G) that the spectral change of Tyr to R-like occurs. The change of Tyr in $\alpha^{Ni}\beta^{Fe}$ is smaller than that in the normal Hb A. This might mean that the ligand binding only to the β heme is not sufficient to induce the complete quaternary structure change.

The behaviors of Tyr and Trp residues at the $\alpha1$-$\beta2$ interface are not synchronous in $\alpha^{Ni}\beta^{Fe}$. This is illustrated in Figure 6 where the peak intensities in the deoxy-minus-CO difference spectra (Figures 4 and 5) of the Y9a bands of Tyr (denoted by Y) and the W16 bands of Trp (denoted by W) are plotted against pH. The right and left panels represent the results for $\alpha^{Ni}\beta^{Fe}$ and $\alpha^{Fe}\beta^{Ni}$, respectively, and the closed and open letters represent the results obtained in the presence and absence of IHP, respectively. The peak intensities increase generally at higher pH, meaning that the protein of the CO-bound form adopts a more R-like structure at higher pH, but the detailed behaviors of Tyr and Trp bands are dissimilar for $\alpha^{Ni}\beta^{Fe}$. In contrast, the behaviors of the Tyr and Trp bands for $\alpha^{deoxy}\beta^{Ni}$ are somewhat alike. Even in this case, however, the spectral changes of Trp and Tyr are not synchronous.

The result from $\alpha^{Ni}\beta^{Fe}$ shows that binding of CO to the β heme promotes the change of Trp to the R-type, but not of Tyr until the pH becomes basic. This means that the change of Trpβ37 to R-like is not always accompanied by the changes of Tyrα42 and Tyrα140, which are known to be quaternary structure sensitive. In other words, the communication route from the β heme to Trpβ37 does not involve Tyrα42 and Tyrα140. In contrast, the result of $\alpha^{Fe}\beta^{Ni}$ shows that binding of CO to the α heme causes almost equally the changes of Tyr and Trp residues. Thus, the information might be communicated to Trpβ37 through Tyrα42 and Tyrα140, supporting Perutz's hypothesis (*2*−*4*) and Ho's communication route (*6*, *7*). In this case, the movement of the Fe−His bond in the α heme is substantial to the quaternary structure transition. Anyway, the communication routes upon the CO binding to the α and β hemes are different from each other.

Relation between Overall Oxygen Affinity and Extent of T → R Quaternary Structural Change at the Half-Ligated State. Oxygen affinity of the Ni−Fe hybrid Hb has been investigated by Shibayama et al. (*8*) who noted that the affinity is sensitive to pH and IHP similar to the case of Hb A. The UVRR spectra of $\alpha^{Ni}\beta^{deoxy}$ and $\alpha^{deoxy}\beta^{Ni}$ at pH 6.7 in the presence of IHP and at pH 8.7 in the absence of IHP are analogous to those of deoxyHb A at pH 6.7 and pH 8.7, respectively. In other words, their quaternary structures in the absence of a ligand are alike and adopt the T structure regardless of pH and IHP. However, oxygen affinities under

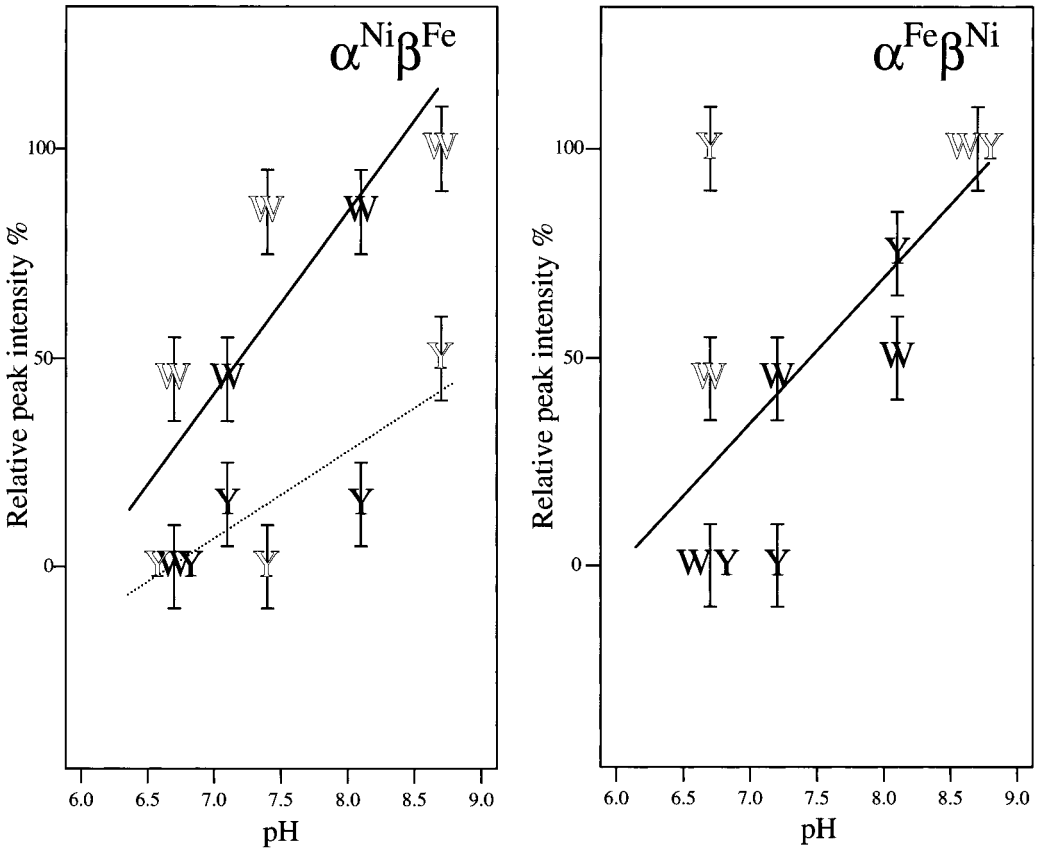

FIGURE 6: The pH dependence of the peak intensities in the deoxy-minus-CO difference spectra shown in Figures 4 and 5 relative to the corresponding peaks in the deoxyHb A-minus-COHb A difference spectra. The left and right panels show the results from $\alpha^{Ni}\beta^{Fe}$ (Figure 4) and $\alpha^{Fe}\beta^{Ni}$ (Figure 5), respectively. "W" and "Y" denote the W16 band of Trp and the Y9a band of Tyr, respectively, and the filled and open letters indicate the values obtained in the presence and absence of IHP, respectively.

the corresponding conditions are largely different. Here we discuss a possible relation of the oxygen affinity with the structural probe at the $\alpha 1$-$\beta 2$ interface.

P_{50} is used as the parameter representing the oxygen affinity, although it may not be correct in the case of $\alpha^{deoxy}\beta^{Ni}$, because of an asymmetrical feature in its oxygen binding curve at higher pH. The UVRR spectroscopic T% is defined for each of Tyr and Trp residues as the ratio of peak intensities in the deoxy-minus-CO difference spectrum to that in the deoxyHb A-minus-COHb A difference spectrum at pH 6.7 in the absence of IHP. This reflects the structural T-like character in the half-ligated state. The results for $\alpha^{Ni}\beta^{Fe}$ and $\alpha^{Fe}\beta^{Ni}$ are plotted against pH in the left and right panels in Figure 7, respectively, where oxygen affinities in the presence and absence of IHP at various pHs reported in ref *8* are designated by the filled and open markers, respectively, with the ordinate scale at the left side. The UVRR spectroscopic T% estimated with the W3, W16, and W18 bands of Trp are denoted by "3", "16", and "18" using the ordinate scale at the right side, and the filled and open letters mean the values obtained in the presence and absence of IHP, respectively. The letters are located at the center of individual error bars.

One may argue that the behavior of the W3 band differs from those of the W16 and W18 bands and that the Raman intensities do not correctly reflect the structure. In fact, the behaviors of the W16 and W18 bands are nearly the same but are slightly different from that of W3. The UVRR spectroscopic T% value for $\alpha^{Ni}\beta^{Fe}$ in the absence of IHP is higher with the W3 band than that with the W16 and W18 bands at pH 6.7 and 7.2, but such differences disappear at pH 8.7. Contrary to this, the UVRR spectroscopic T% values for $\alpha^{Fe}\beta^{Ni}$ in the presence of IHP are lower with the W3 band than those with the W16 and W18 bands at pH 6.7 and 8.1, while such a difference is absent at pH 7.4. One of the reasons for such discrepancy lies in the character of sensitivity. For the W3 band a frequency is sensitive to the $\chi^{2,1}$ angle, but for W16 and W18 bands Raman intensity is sensitive to hydrophobicity around the residue. Thus, the inclusion of the contribution from Trpα14 and Trpβ15 is different between the W3 and W16 (or W18) bands. The other reason is rather technical, that is, incorrect drawing of a baseline. Considering these uncertainties, we can conclude that the overall behaviors of both the W3 and W16 (or W18) bands are qualitatively similar.

The plots in Figure 7 mean that the trend of Raman markers in the absence of IHP appears to parallel that of open markers of oxygen affinity, suggesting that the T-like character of Trpβ37 in the half-liganded state is directly related to the overall oxygen affinity. In the presence of IHP, the oxygen affinity is generally lower and the T% values from Raman spectra are higher than those in its absence, although the behaviors are complicated. The correlation between the structural parameter (UVRR) and the oxygen affinity seems to be better for $\alpha^{Ni}\beta^{Fe}$ than for $\alpha^{Fe}\beta^{Ni}$, and IHP effects are clearer in the oxygen affinity than structural parameters. Note that P_{50} is an average character of K_1 and K_2, but the Raman parameters represent the extent of

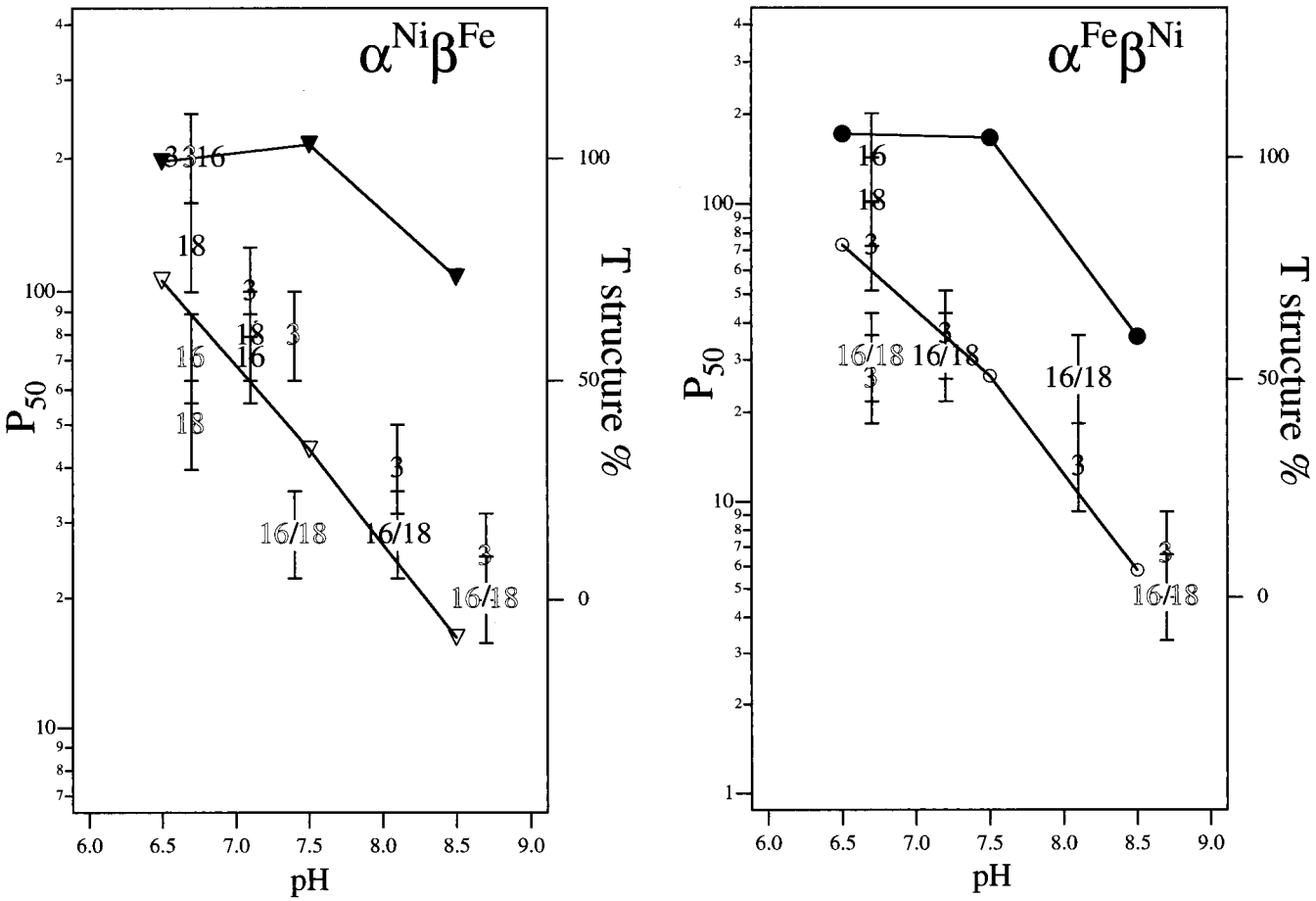

FIGURE 7: The relation between oxygen affinity (P_{50}) and the Raman T-like nature of tryptophan. P_{50} of $\alpha^{Ni}\beta^{Fe}$ (∇) and $\alpha^{Fe}\beta^{Ni}$ (O) reported (ref 8) are plotted with the ordinate scale of the left side. The percentage values of T-like nature in the half-liganded form are plotted with the ordinate scale at the right side, in which the values obtained from the W3, W16, and W18 bands of Trp are represented simply with "3", "16", and "18", respectively. The position of the marker denotes the center of individual error bars. The filled and open letters (or symbols) indicate the values obtained in the presence and absence of IHP, respectively.

structural change at the half-liganded stage and thus are related to K_3. Similar plots for Tyr bands (not shown) were more complicated, but it is understood from the fact that the behaviors of Tyr and Trp are not concerted.

Correlation between Fe−His Bond and the α1-β2 Interface Contacts. In the previous RR study on NOHb, we proposed that although the movement of the proximal His due to the out-of-plane displacement of Fe in the α subunit is substantial to the quaternary structure change, it is not a sole origin, and that the movement of the proximal His in the β subunit also contributes to it (*19*). In the case of $\alpha^{NO}\beta^{deoxy}$, binding of CO or NO to the β heme affects Tyr and Trp residues. For $\alpha^{Ni}\beta^{deoxy}$, however, the change of Trp occurs in a manner similar to that in $\alpha^{NO}\beta^{deoxy}$, but the change of Tyr is much smaller. The two proteins are common with regard to the fact that the Fe−His or Ni−His bond is cleaved in the α subunit. Binding of CO to the α heme in $\alpha^{deoxy}\beta^{Ni}$ affects Tyr and Trp residues, but binding of NO to the α heme in $\alpha^{deoxy}\beta^{deoxy}$ (deoxyHb A) affects neither Tyr nor Trp residues. Their behaviors in the Ni−Fe hybrid Hb are different from those in NOHb regarding the difference in the R-like shifts of Tyr between $\alpha^{NO}\beta^{deoxy}$ and $\alpha^{CO}\beta^{Ni}$ and also that between NOHb ($\alpha^{NO}\beta^{NO}$) and $\alpha^{Ni}\beta^{CO}$. These differences are discussed below.

It is well-known that the physicochemical effects of ligand binding are significantly different between CO and NO as a ligand. Six coordination is more favorable than five coordination with CO, but it is opposite with NO (*46*−*49*). The Fe−His bond in the α subunit of $\alpha^{NO}\beta^{deoxy}$ is cleaved at lower pH, but it recovers at higher pH where six coordination is attained (*50*−*55*). This situation of $\alpha^{NO}\beta^{deoxy}$ at higher pH is apparently similar to that in $\alpha^{CO}\beta^{Ni}$ at pH 6.7 in the absence of IHP in the sense that the α heme adopts six coordination. Nevertheless, in $\alpha^{NO}\beta^{deoxy}$ at pH 8.8, both Tyr and Trp residues remain in the T structure, while in $\alpha^{CO}\beta^{Ni}$ at pH 6.7 in the absence of IHP, Tyr is of R type and Trp is of half R-type. We attribute this to the difference in the metal-His bonding (*19*). The metal-His distance in the four-coordinated α subunit of $\alpha^{Ni}\beta^{CO}$ is sufficiently long (320 pm) (*16*). Table 1 summarizes the Fe−ligand and Fe−His bond lengths and the Fe−Ct distances determined by X-ray crystallographic analysis (*56*−*65*). The Fe−His distance in the α subunit is 216 pm or longer for the T state, whereas it is shorter (194 pm) for the R state, meaning that the Fe atom draws the proximal His toward the heme less in the T than R state.

Figure 8 schematically illustrates an empirical relation between the positions of the proximal His in the α subunit and the quaternary structures of the tetramer. The X-ray crystallographic analysis determined that the Fe−His distances of oxyT and oxyR Hbs are ca. 218 (60, Figure 8D) and 194 pm (65, Figure 8E), respectively. The former is close

Table 1: Structural Parameters of the Heme Proximity for NO-Bound Heme Proteins and Related Model Compounds Determined by X-ray Crystallographic Analysis

		Fe−NO(O_2)[a]		Fe−His[b]		Fe- - -Ct[c,d]		
		α	β	α	β	α	β	ref
5-coordinate	Fe(TPP)(NO)	171.7				−21.1[d]		*56*
	Fe(OEP)(NO)	172.2				−29[d]		*57*
	Fe(TpivP)(NO)	172				−26.0[c]		*58*
	deoxyHbA			216	209	40[c]	36[c]	*59*
6-coordinate	T(α-oxy)Hb	180	200	α_1 218	217	18[c]	43[c]	*60*
				α_1 232				
	Fe(TPP)(NO)(N-MeIm)	174.3		218		7[c]		*61*
	SNO−NOHb	174	175	228	228			62
	NOLb	172		220		2[c]		63
	NOMb(SW)	189		218		0[d]		64
	OxyHbA	166	187	194	207	−12[c]	11[c]	65

[a] Fe−N(NO) or Fe−O(O_2) distance in pm unit. [b] Fe−N(histidine) distance in pm unit. [c] Ct is a center of porphyrin in the plane of four pyrrole nitrogen atoms. The out-of-plane displacement of Fe is represented in pm unit. "−" is the direction toward distal histidine. [d] Same as footnote c except that Ct is a center of mean plane of porphyrin.

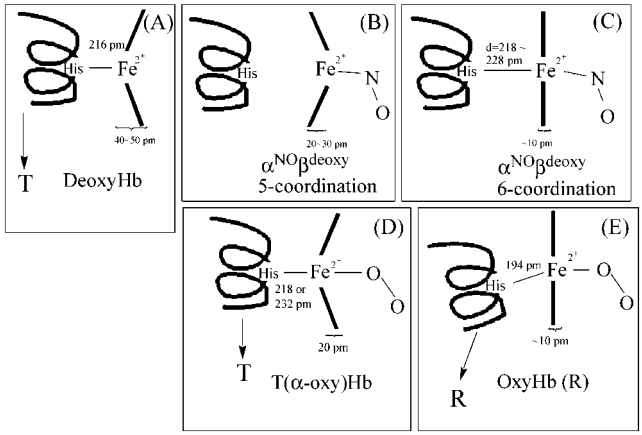

FIGURE 8: Schematic illustration of the position of the proximal histidine in the α subunit for various forms. The Fe−His distance is transferred from each X-ray crystallographic analysis quoted. (A) deoxyHb A (ref *59*), (B) $\alpha^{NO}\beta^{deoxy}$ at pH 5.6, +IHP, (C) $\alpha^{NO}\beta^{deoxy}$ at pH 8.8 in the absence of IHP, (D) α-oxy form in the T structure Hb (ref *60*), and (E) oxyHb A in the normal R structure (ref *65*).

to that in deoxyHb A (59, Figure 8A). Scheidt and coworkers (*57*, *58*, *61*) noted that the Fe−NO distance is hardly different between the five- and six-coordinated ferrous NO porphyrins (172 and 174 pm, respectively). Since the local structure around the α-heme of horse Hb (*62*) is similar to that of Fe(TPP)(NO)(N-MeIm) (*61*), the Fe−His distance in the six-coordinated Hb would be close to the Fe−(N-MeIm) distance (218 pm) of Fe(TPP)(NO)(N-MeIm), which is depicted in Figure 8C. This distance is similar to that of the oxyT Hb structure (Figure 8D) rather than that of oxyR Hb (Figure 8E). It means that the proximal His is located at the position of T quaternary structure. Therefore, even if the Fe−His distance becomes further longer due to the out-of-plane movement of Fe toward the opposite direction as illustrated in Figure 8B, the position of proximal His would remain unaltered (stay at the position of T).

Communication Route of Ligand Binding between the α *and* β *Subunits.* The aforementioned second problem is the difference in the spectral changes of Tyr bands between NOHb ($\alpha^{NO}\beta^{NO}$) and $\alpha^{Ni}\beta^{CO}$. The change of Tyr bands toward R-like was not observed for $\alpha^{Ni}\beta^{CO}$ at neutral pH, while it was almost fully changed to R-like in $\alpha^{NO}\beta^{NO}$ even at lower pH (pH 5.5) in the presence of IHP (*19*). Their structural features before the ligand binding to the β heme are alike, that is, the Fe−His bond is cleaved in the α subunit for both $\alpha^{Ni}\beta^{deoxy}$ at pH 6.7 in the absence of IHP and $\alpha^{NO}\beta^{deoxy}$ at pH 5.5 in the presence of IHP (*8*, *46*−*49*, *53*−*55*). The clearly different point between $\alpha^{NO}\beta^{deoxy}$ and $\alpha^{Ni}\beta^{deoxy}$ is whether a ligand (NO) is present or absent in the heme pocket of the α subunit. It is well-known that the heme-bound NO forms a hydrogen bond with Hisα58 of the E-helix (*66*). Tomita et al. (*67*) also confirmed it with mutant NOMbs by observing the ν_{NO} frequency, which is sensitive to the hydrogen bonding from the protein moiety to NO. This suggests the existence of a hydrogen bonding network from Fe−NO···Hisα58 to the subunit interface, and a similar network will be present in the O_2-bound form of Hb A. There is no such a network between the α heme and the α1-β2 subunit interface in $\alpha^{Ni}\beta^{CO}$.

In a previous study, we assumed the communication route of quaternary structure change from the β heme to the subunit interface as follows (*19*): (1) Hisβ92 (F8) → Valβ98 (FG5) → Aspβ99 (G1) → Tyrα42 (C7) → Argβ40 (C6) → Argα92 (FG4) → Valα93 (FG5) → Tyrα140 (HC2) → Trpβ37 (C3), and (2) Hisβ92 (F8) → Valβ98 (FG5) → Tyrβ145 (HC2). Roughly speaking, these are the reversed course of the communication route from the α heme to the β heme proposed by Ho (*7*). These routes assumed that Tyrβ145 and Tyrα42 would be more sensitively influenced by ligand binding than Trpβ37, and that therefore the ligand binding to the β heme promotes the change of Tyr toward R-like. However, the result on $\alpha^{Ni}\beta^{CO}$ at pH 6.7 in the absence of IHP means that Tyr residues remain in the T structure after binding of a ligand to the β heme (Figure 4C). Therefore, although the behavior of Trp upon ligand binding to the β-heme is almost the same between $\alpha^{NO}\beta^{NO}$ and $\alpha^{Ni}\beta^{CO}$, that of Tyr is different. In this regard, we supplement our previous conclusion on NOHb by noting that the Tyr routes mentioned above are contributing but its relative importance may depend on the existence of the ligand−protein hydrogen bonding network such as the Fe−NO···Hisα58.

In conclusion, UVRR spectroscopic studies on the Ni−Fe hybrid Hb demonstrated the differences in structural changes at the α1-β2 subunit interface between ligand binding to the α and β hemes. Ligation to the α heme affects both Tyr and Trp residues, but ligation to the β heme affects only Trp residues. The differences in behaviors between Trp and Tyr residues as well as between the α and β subunits

are stressed. Comparison of the results on $\alpha^{Ni}\beta^{CO}$ with the results from our previous study on $\alpha^{NO}\beta^{CO}$ and $\alpha^{NO}\beta^{NO}$ suggests that the structure of interface Tyr residues is related to a structure of distal His (Hisα58) in the α subunit, which depends on the presence or absence of a hydrogen bond network between the bound ligand and the distal His. In $\alpha^{Ni}\beta^{CO}$, the T to R change of Trp residues proceeds smoothly as pH is raised but that of Tyr does not. In $\alpha^{CO}\beta^{Ni}$, on the other hand, the T to R changes of Trp and Tyr residues take place to a similar extent as the pH is raised. IHP retards the T to R change of Tyr, particularly at lower pH. Finally, it is noted that $\alpha^{Ni}\beta^{CO}$ and $\alpha^{CO}\beta^{Ni}$ at pH 6.7 in the presence of IHP stay in the complete T quaternary structure, indicating its unusual stability of the T structure.

REFERENCES

1. Monod, J., Wyman, J., and Changeux, J. P. (1965) *J. Mol. Biol. 12*, 88−118.
2. Perutz, M. F. (1970) *Nature 228*, 726−739.
3. Perutz, M. F. (1979) *Annu. Rev. Biochem. 48*, 327−386.
4. Perutz, M. F., Fermi, G., Luisi, B., Shaanan, B., and Liddington, R. C. (1987) *Acc. Chem. Res. 20*, 309−321.
5. Baldwin, J., and Chothia, C. (1979) *J. Mol. Biol. 129*, 175−220.
6. Fung, L. W.-M., and Ho, C. (1975) *Biochemistry 14*, 2526−2535.
7. Ho, C. (1992) *Adv. Protein Chem. 43*, 152−312.
8. Shibayama, N., Morimoto, H., and Miyazaki, G. (1986) *J. Mol. Biol. 192*, 323−329.
9. Shibayama, N., Inubushi, T., Morimoto, H., and Yonetani, T. (1987) *Biochemistry 26*, 2194−2201.
10. Inubushi, T., Ikeda-Saito, M., and Yonetani, T. (1987) *Biochemistry 22*, 2904−2907.
11. Venkatesh, B., Hori, H., Miyazaki, G., Nagatomo, S. Kitagawa, T., and Morimoto, H. (2002) *J. Inorg. Biochem. 88*, 310−315.
12. Miyazaki, G., Morimoto, H., Yun, K.-M., Park, S.-Y., Nakagawa, A., Minagawa, H., and Shibayama, N. (1999) *J. Mol. Biol. 292*, 1121−1136.
13. Park, S.-Y., Nakagawa, A., and Morimoto, H. (1996) *J. Mol. Biol. 255*, 726−734.
14. Arnone, A., Rogers, P., Blough, N. V., McGourty, J. L., and Hoffman, B. M. (1986) *J. Mol. Biol. 188*, 693−706.
15. Unzai, S., Eich, R., Shibayama, N., Olson, J. S., and Morimoto, H. (1998) *J. Biol. Chem. 273*, 23150−23159.
16. Luisi, B., Liddington, B., Fermi., G., and Shibayama, N. (1990) *J. Mol. Biol. 214*, 7−14.
17. Luisi, B., and Shibayama, N. (1989) *J. Mol. Biol. 206*, 723−736.
18. Shibayama, N., Yonetani, T., Regan, R. M., and Gibson, Q. H. (1995) *Biochemistry 34*, 14658−14667.
19. Nagatomo, S., Nagai, M., Tsuneshige, A., Yonetani, T., and Kitagawa, T. (1999) *Biochemistry 38*, 9659−9666.
20. Harada, I., Miura, T., and Takeuchi, H. (1986) *Spectrochim. Acta 42A*, 307−312.
21. Kitagawa, T. (1992) *Prog. Biophys. Mol. Biol. 58*, 1−18.
22. Rodgers, K. R., Su, C., Subramaniam, S., and Spiro, T. G. (1992) *J. Am. Chem. Soc. 114*, 3697−3709.
23. Rodgers, K. R., and Spiro, T. G. (1992) *Science 265*, 1697−1699.
24. Nagai, M., Kaminaka, S, Ohba, Y, Nagai, Y, Mizutani, Y., and Kitagawa, T. (1995) *J. Biol. Chem. 270*, 1636−1642.
25. Nagai, M., Imai, K., Kaminaka, S., Mizutani, Y., and Kitagawa, T. (1996) *J. Mol. Struct. 379*, 65−75.
26. Nagai, M., Wajcman, H., Lahary, A., Nakatsukasa, T., Nagatomo, S., and Kitagawa, T. (1999) *Biochemistry 38*, 1243−1251.
27. Huang, S., Peterson, E. S., Ho, C., and Friedman, J. M. (1997) *Biochemistry 36*, 6197−6206.
28. Huang, J., Juszczak, L., Peterson, E. S., Shannon, C. F., Yang, M., Huang, S., Vidugiris, G. V. A., and Friedman, J. M. (1999) *Biochemistry 38*, 4514−4525.
29. Hu, X., and Spiro, T. G. (1997) *Biochemistry 36*, 15701−15712.
30. Hu, X., Rodgers, K. R., Mukerji, I., and Spiro, T. G. (1999) *Biochemistry 38*, 3462−3467.
31. Peterson, E. S., and Friedman, J. M. (1998) *Biochemistry 37*, 4346−4357.
32. Nagai, M., Nishibu, M., Sugita, Y., Yoneyama, Y., Jones, R. T., and Gordon, S. (1975) *J. Biol. Chem. 250*, 3169−3173.
33. Kaminaka, S., and Kitagawa, T. (1995) *Appl. Spectrosc. 49*, 685−687.
34. Ogoshi, H., Watanabe, E., Yoshida, Z., Kincaid, J., and Nakamoto, K. (1973) *J. Am. Chem. Soc. 95*, 2845.
35. Song, S., and Asher, S. A. (1991) *Biochemistry 30*, 1199−1205.
36. Kaminaka, S., and Kitagawa, T. (1992) *Appl. Spectrosc. 46*, 1804−1808.
37. Dudik, J. M., Johnson, C. R., and Asher, S. A. (1985) *J. Chem. Phys. 82*, 1732−1740.
38. Miura, T., Takeuchi, H., and Harada, I. (1988) *Biochemistry 27*, 88−94.
39. Miura, T., Takeuchi, H., and Harada, I. (1989) *J. Raman Spectrosc. 20*, 667−671.
40. Chi, Z., and Asher, S. A. (1998) *J. Phys. Chem. B. 102*, 9595−9602.
41. Matsuno, M., and Takeuchi, H. (1998) *Bull. Chem., Soc., Jpn. 71*, 851−857.
42. Harada, I., and Takeuchi, H. (1986) *Adv. Spectrosc. 13*, 113−175.
43. Kaminaka, S., and Kitagawa, T. (1992) *J. Am. Chem. Soc. 114*, 3256−3260.
44. Kitagawa, T., Abe, M., and Ogoshi, H. (1978) *J. Phys. Chem. 69*, 4516−4525.
45. Abe, M., Kitagawa, T., and Kyogoku, Y. (1978) *J. Phys. Chem. 69*, 4526−4534.
46. Rougee, M., and Brault, D. (1975) *Biochemistry 14*, 4100−4106.
47. Rose, E. J., and Hoffman, B. M. (1983) *J. Am. Chem. Soc. 105*, 2866−2873.
48. Gibson, Q. H., and Roughton, F. J. W. (1957) *J. Physiol. 136*, 507−526.
49. Antonini, E., and Brunori, M. (1971) *Hemoglobin and Myoglobin in their Reactions with Ligands*, North-Holland, Amsterdam.
50. Yonetani, T., Tsuneshige, A., Zhou, Y., and Chen, X. (1998) *J. Biol. Chem. 273*, 20323−20333.
51. Perutz, M. F., Kilmartin, J. V., Nagai, K., Szabo, A., and Simon, S. R. (1976) *Biochemistry 15*, 378−387.
52. Salhany, J. M., Ogawa, S., and Shulman, R. G., (1975) *Biochemistry 14*, 2180−2190.
53. Nagai, K., Hori, H., Yoshida, S., Sakamoto, H., and Morimoto, H. (1978) *Biochim. Biophys. Acta 532*, 17−28.
54. Hille, R., Olson, J. S., and Palmer, G. (1979) *J. Biol. Chem. 254*, 12110−12120.
55. Nagai, K., Welborn, C., Dolphin D., and Kitagawa, T. (1980) *Biochemistry 19*, 4755−4761.
56. Scheidt, W. R., and Frisse, M. E. (1975) *J. Am. Chem. Soc. 97*, 17−21.
57. Ellison, M. K., and Scheidt, W. R. (1975) *J. Am. Chem. Soc. 119*, 7404−7405.
58. Nasri, H., Haller, K. J., Wang, Y., Huynh, B. H., and Scheidt, W. R. (1992) *Inorg. Chem. 31*, 3459−3467.
59. Fermi, G., Perutz, M. F., Shaanan, B., and Fourme, R. (1984) *J. Mol. Biol. 175*, 159−174.
60. Liddington, R., Derewenda, Z., Dodson, E., Hubbard, R., and Dodson, G. (1992) *J. Mol. Biol. 228*, 551−579.
61. Scheidt, W. R., and Piciulo, L. (1976) *J. Am. Chem. Soc. 98*, 1913−1919.
62. Chan, N.-L., Rogers, P. H., and Arnone, A. (1998) *Biochemistry 37*, 16459−16464.
63. Harutyunyan, E. H., Safonova, T. N., Kuranova, I. P., Popov, A. N., Teplyakov, A. V., Obmolova, G. V., Vainshtein, B. K., Dodson, G. G., and Wilson, J. C. (1996) *J. Mol. Biol. 264*, 152−161.
64. Brucker, E. A., Olson, J. S., Ikeda-Saito, M., and Phillips, G. N., Jr. (1998) *Proteins 30*, 352−356.
65. Shaanan, B. (1983) *J. Mol. Biol. 171*, 31−59.
66. Olson, J. S., and Phillips, G. N. Jr. (1997) *J. Bio. Inorg. Chem. 2*, 544−552.
67. Tomita, T., Hirota, S., Ogura, T., Olson, J. S., and Kitagawa, T. (1999*) J. Phys. Chem. B 103*, 7044−7054.

BI0200460